arXiv:nucl-ex/0408007v1 7 Aug 2004

Jet Structure of Baryon Excess in Au+Au Collisions at $\sqrt{s_{NN}}$ =200 GeV

S.S. Adler,[5] S. Afanasiev,[20] C. Aidala,[5,10] N.N. Ajitanand,[47] Y. Akiba,[23,42] A. Al-Jamel,[37] J. Alexander,[47] R. Amirikas,[14] K. Aoki,[27] L. Aphecetche,[49] R. Armendariz,[37] S.H. Aronson,[5] R. Averbeck,[48] T.C. Awes,[38] R. Azmoun,[48] V. Babintsev,[17] A. Baldisseri,[11] K.N. Barish,[6] P.D. Barnes,[30] B. Bassalleck,[36] S. Bathe,[6,33] S. Batsouli,[10] V. Baublis,[41] F. Bauer,[6] A. Bazilevsky,[5,17,43] S. Belikov,[19,17] Y. Berdnikov,[44] S. Bhagavatula,[19] M.T. Bjorndal,[10] J.G. Boissevain,[30] H. Borel,[11] S. Borenstein,[28] M.L. Brooks,[30] D.S. Brown,[37] N. Bruner,[36] D. Bucher,[33] H. Buesching,[5,33] V. Bumazhnov,[17] G. Bunce,[5,43] J.M. Burward-Hoy,[29,30,48] S. Butsyk,[48] X. Camard,[49] J.-S. Chai,[21] P. Chand,[4] W.C. Chang,[2] S. Chernichenko,[17] C.Y. Chi,[10] J. Chiba,[23] M. Chiu,[10] I.J. Choi,[56] J. Choi,[22] R.K. Choudhury,[4] T. Chujo,[5] V. Cianciolo,[38] Y. Cobigo,[11] B.A. Cole,[10] M.P. Comets,[39] P. Constantin,[19] M. Csanád,[13] T. Csörgő,[24] J.P. Cussonneau,[49] D. d'Enterria,[10] D.G. d'Enterria,[49] K. Das,[14] G. David,[5] F. Deák,[13] H. Delagrange,[49] A. Denisov,[17] A. Deshpande,[43] E.J. Desmond,[5] A. Devismes,[48] O. Dietzsch,[45] J.L. Drachenberg,[1] O. Drapier,[28] A. Drees,[48] K.A. Drees,[5] R. du Rietz,[32] A. Durum,[17] D. Dutta,[4] V. Dzhordzhadze,[50] Y.V. Efremenko,[38] K. El Chenawi,[53] A. Enokizono,[16] H. En'yo,[42,43] B. Espagnon,[39] S. Esumi,[52] L. Ewell,[5] D.E. Fields,[36,43] C. Finck,[49] F. Fleuret,[28] S.L. Fokin,[26] B.D. Fox,[43] Z. Fraenkel,[55] J.E. Frantz,[10] A. Franz,[5] A.D. Frawley,[14] Y. Fukao,[27,42,43] S.-Y. Fung,[6] S. Gadrat,[31] S. Garpman,[32,*] M. Germain,[49] T.K. Ghosh,[53] A. Glenn,[50] G. Gogiberidze,[50] M. Gonin,[28] J. Gosset,[11] Y. Goto,[42,43] R. Granier de Cassagnac,[28] R. Granier de Cassagnac,[28] N. Grau,[19] S.V. Greene,[53] M. Grosse Perdekamp,[18,43] W. Guryn,[5] H.-Å. Gustafsson,[32] T. Hachiya,[16] J.S. Haggerty,[5] H. Hamagaki,[8] A.G. Hansen,[30] E.P. Hartouni,[29] M. Harvey,[5] K. Hasuko,[42] R. Hayano,[8] N. Hayashi,[42] X. He,[15] M. Heffner,[29] T.K. Hemmick,[48] J.M. Heuser,[42,48] M. Hibino,[54] P. Hidas,[24] H. Hiejima,[18] J.C. Hill,[19] R. Hobbs,[36] W. Holzmann,[47] K. Homma,[16] B. Hong,[25] A. Hoover,[37] T. Horaguchi,[42,43,51] T. Ichihara,[42,43] V.V. Ikonnikov,[26] K. Imai,[27,42] M. Inaba,[52] M. Inuzuka,[8] D. Isenhower,[1] L. Isenhower,[1] M. Ishihara,[42] M. Issah,[47] A. Isupov,[20] B.V. Jacak,[48] W.Y. Jang,[25] Y. Jeong,[22] J. Jia,[48] O. Jinnouchi,[42,43] B.M. Johnson,[5] S.C. Johnson,[29] K.S. Joo,[34] D. Jouan,[39] F. Kajihara,[8] S. Kametani,[8,54] N. Kamihara,[42,51] M. Kaneta,[43] J.H. Kang,[56] S.S. Kapoor,[4] K. Katou,[54] T. Kawabata,[8] A. Kazantsev,[26] S. Kelly,[9,10] B. Khachaturov,[55] A. Khanzadeev,[41] J. Kikuchi,[54] D.H. Kim,[34] D.J. Kim,[56] D.W. Kim,[22] E. Kim,[46] G.-B. Kim,[28] H.J. Kim,[56] E. Kinney,[9] W.W. Kinnison,[30] A. Kiss,[13] E. Kistenev,[5] A. Kiyomichi,[42,52] K. Kiyoyama,[35] C. Klein-Boesing,[33] H. Kobayashi,[42,43] L. Kochenda,[41] V. Kochetkov,[17] D. Koehler,[36] T. Kohama,[16] R. Kohara,[16] B. Komkov,[41] M. Konno,[52] M. Kopytine,[48] D. Kotchetkov,[6] A. Kozlov,[55] P.J. Kroon,[5] C.H. Kuberg,[1,30] G.J. Kunde,[30] K. Kurita,[42,43] Y. Kuroki,[52] M.J. Kweon,[25] Y. Kwon,[56] G.S. Kyle,[37] R. Lacey,[47] V. Ladygin,[20] J.G. Lajoie,[19] Y. Le Bornec,[39] A. Lebedev,[19,26] S. Leckey,[48] D.M. Lee,[30] S. Lee,[22] M.J. Leitch,[30] M.A.L. Leite,[45] X.H. Li,[6] H. Lim,[46] A. Litvinenko,[20] M.X. Liu,[30] Y. Liu,[39] C.F. Maguire,[53] Y.I. Makdisi,[5] A. Malakhov,[20] V.I. Manko,[26] Y. Mao,[7,40,42] G. Martinez,[49] M.D. Marx,[48] H. Masui,[52] F. Matathias,[48] T. Matsumoto,[8,54] M.C. McCain,[1] P.L. McGaughey,[30] E. Melnikov,[17] F. Messer,[48] Y. Miake,[52] J. Milan,[47] T.E. Miller,[53] A. Milov,[48,55] S. Mioduszewski,[5] R.E. Mischke,[30] G.C. Mishra,[15] J.T. Mitchell,[5] A.K. Mohanty,[4] D.P. Morrison,[5] J.M. Moss,[30] F. Mühlbacher,[48] D. Mukhopadhyay,[55] M. Muniruzzaman,[6] J. Murata,[42,43] S. Nagamiya,[23] J.L. Nagle,[9,10] T. Nakamura,[16] B.K. Nandi,[6] M. Nara,[52] J. Newby,[50] P. Nilsson,[32] A.S. Nyanin,[26] J. Nystrand,[32] E. O'Brien,[5] C.A. Ogilvie,[19] H. Ohnishi,[5,42] I.D. Ojha,[3,53] H. Okada,[27,42] K. Okada,[42,43] M. Ono,[52] V. Onuchin,[17] A. Oskarsson,[32] I. Otterlund,[32] K. Oyama,[8] K. Ozawa,[8] D. Pal,[55] A.P.T. Palounek,[30] V. Pantuev,[48] V.S. Pantuev,[48] V. Papavassiliou,[37] J. Park,[46] W.J. Park,[25] A. Parmar,[36] S.F. Pate,[37] H. Pei,[19] T. Peitzmann,[33] V. Penev,[20] J.-C. Peng,[18,30] H. Pereira,[11] V. Peresedov,[20] A. Pierson,[36] C. Pinkenburg,[5] R.P. Pisani,[5] F. Plasil,[38] M.L. Purschke,[5] A.K. Purwar,[48] J. Qualls,[1] J. Rak,[19] I. Ravinovich,[55] K.F. Read,[38,50] M. Reuter,[48] K. Reygers,[33] V. Riabov,[41,44] Y. Riabov,[41] G. Roche,[31] A. Romana,[28] M. Rosati,[19] S. Rosendahl,[32] P. Rosnet,[31] V.L. Rykov,[42] S.S. Ryu,[56] M.E. Sadler,[1] N. Saito,[27,42,43] T. Sakaguchi,[8,54] M. Sakai,[35] S. Sakai,[52] V. Samsonov,[41] L. Sanfratello,[36] R. Santo,[33] H.D. Sato,[27,42] S. Sato,[5,52] S. Sawada,[23] Y. Schutz,[49] V. Semenov,[17] R. Seto,[6] M.R. Shaw,[1,30] T.K. Shea,[5] I. Shein,[17] T.-A. Shibata,[42,51] K. Shigaki,[16,23] T. Shiina,[30] M. Shimomura,[52] A. Sickles,[48] C.L. Silva,[45] D. Silvermyr,[30,32] K.S. Sim,[25] J. Simon-Gillo,[30] C.P. Singh,[3] V. Singh,[3] M. Sivertz,[5] A. Soldatov,[17] R.A. Soltz,[29] W.E. Sondheim,[30] S. Sorensen,[50] S.P. Sorensen,[50] I.V. Sourikova,[5] F. Staley,[11] P.W. Stankus,[38] E. Stenlund,[32] M. Stepanov,[37] A. Ster,[24] S.P. Stoll,[5] T. Sugitate,[16] J.P. Sullivan,[30] S. Takagi,[52] E.M. Takagui,[45] A. Taketani,[42,43] M. Tamai,[54] K.H. Tanaka,[23] Y. Tanaka,[35] K. Tanida,[42] M.J. Tannenbaum,[5] A. Taranenko,[47] P. Tarján,[12] J.D. Tepe,[1,30] T.L. Thomas,[36] M. Togawa,[27,42] J. Tojo,[27,42] H. Torii,[27,42,43] R.S. Towell,[1] V-N. Tram,[28] I. Tserruya,[55] Y. Tsuchimoto,[16] H. Tsuruoka,[52] S.K. Tuli,[3]

H. Tydesjö,[32] N. Tyurin,[17] T.J. Uam,[34] H.W. van Hecke,[30] J. Velkovska,[5,48] M. Velkovsky,[48] V. Veszprémi,[12] L. Villatte,[50] A.A. Vinogradov,[26] M.A. Volkov,[26] E. Vznuzdaev,[41] X.R. Wang,[15] Y. Watanabe,[42,43] S.N. White,[5] N. Willis,[39] F.K. Wohn,[19] C.L. Woody,[5] W. Xie,[6] Y. Yang,[7] A. Yanovich,[17] S. Yokkaichi,[42,43] G.R. Young,[38] I.E. Yushmanov,[26] W.A. Zajc,[10,†] C. Zhang,[10] S. Zhou,[7] S.J. Zhou,[55] J. Zimányi,[24] L. Zolin,[20] and X. Zong[19]

(PHENIX Collaboration)

[1]*Abilene Christian University, Abilene, TX 79699, USA*
[2]*Institute of Physics, Academia Sinica, Taipei 11529, Taiwan*
[3]*Department of Physics, Banaras Hindu University, Varanasi 221005, India*
[4]*Bhabha Atomic Research Centre, Bombay 400 085, India*
[5]*Brookhaven National Laboratory, Upton, NY 11973-5000, USA*
[6]*University of California - Riverside, Riverside, CA 92521, USA*
[7]*China Institute of Atomic Energy (CIAE), Beijing, People's Republic of China*
[8]*Center for Nuclear Study, Graduate School of Science, University of Tokyo, 7-3-1 Hongo, Bunkyo, Tokyo 113-0033, Japan*
[9]*University of Colorado, Boulder, CO 80309*
[10]*Columbia University, New York, NY 10027 and Nevis Laboratories, Irvington, NY 10533, USA*
[11]*Dapnia, CEA Saclay, F-91191, Gif-sur-Yvette, France*
[12]*Debrecen University, H-4010 Debrecen, Egyetem tér 1, Hungary*
[13]*ELTE, Eötvös Loránd University, H - 1117 Budapest, Pázmány P. s. 1/A, Hungary*
[14]*Florida State University, Tallahassee, FL 32306, USA*
[15]*Georgia State University, Atlanta, GA 30303, USA*
[16]*Hiroshima University, Kagamiyama, Higashi-Hiroshima 739-8526, Japan*
[17]*Institute for High Energy Physics (IHEP), Protvino, Russia*
[18]*University of Illinois at Urbana-Champaign, Urbana, IL 61801*
[19]*Iowa State University, Ames, IA 50011, USA*
[20]*Joint Institute for Nuclear Research, 141980 Dubna, Moscow Region, Russia*
[21]*KAERI, Cyclotron Application Laboratory, Seoul, South Korea*
[22]*Kangnung National University, Kangnung 210-702, South Korea*
[23]*KEK, High Energy Accelerator Research Organization, Tsukuba-shi, Ibaraki-ken 305-0801, Japan*
[24]*KFKI Research Institute for Particle and Nuclear Physics (RMKI), H-1525 Budapest 114, POBox 49, Hungary*
[25]*Korea University, Seoul, 136-701, Korea*
[26]*Russian Research Center "Kurchatov Institute", Moscow, Russia*
[27]*Kyoto University, Kyoto 606, Japan*
[28]*Laboratoire Leprince-Ringuet, Ecole Polytechnique, CNRS-IN2P3, Route de Saclay, F-91128, Palaiseau, France*
[29]*Lawrence Livermore National Laboratory, Livermore, CA 94550, USA*
[30]*Los Alamos National Laboratory, Los Alamos, NM 87545, USA*
[31]*LPC, Université Blaise Pascal, CNRS-IN2P3, Clermont-Fd, 63177 Aubiere Cedex, France*
[32]*Department of Physics, Lund University, Box 118, SE-221 00 Lund, Sweden*
[33]*Institut für Kernphysik, University of Muenster, D-48149 Muenster, Germany*
[34]*Myongji University, Yongin, Kyonggido 449-728, Korea*
[35]*Nagasaki Institute of Applied Science, Nagasaki-shi, Nagasaki 851-0193, Japan*
[36]*University of New Mexico, Albuquerque, NM 87131, USA*
[37]*New Mexico State University, Las Cruces, NM 88003, USA*
[38]*Oak Ridge National Laboratory, Oak Ridge, TN 37831, USA*
[39]*IPN-Orsay, Universite Paris Sud, CNRS-IN2P3, BP1, F-91406, Orsay, France*
[40]*Peking University, Beijing, People's Republic of China*
[41]*PNPI, Petersburg Nuclear Physics Institute, Gatchina, Russia*
[42]*RIKEN (The Institute of Physical and Chemical Research), Wako, Saitama 351-0198, JAPAN*
[43]*RIKEN BNL Research Center, Brookhaven National Laboratory, Upton, NY 11973-5000, USA*
[44]*St. Petersburg State Technical University, St. Petersburg, Russia*
[45]*Universidade de São Paulo, Instituto de Física, Caixa Postal 66318, São Paulo CEP05315-970, Brazil*
[46]*System Electronics Laboratory, Seoul National University, Seoul, South Korea*
[47]*Chemistry Department, Stony Brook University, Stony Brook, SUNY, NY 11794-3400, USA*
[48]*Department of Physics and Astronomy, Stony Brook University, SUNY, Stony Brook, NY 11794, USA*
[49]*SUBATECH (Ecole des Mines de Nantes, CNRS-IN2P3, Université de Nantes) BP 20722 - 44307, Nantes, France*
[50]*University of Tennessee, Knoxville, TN 37996, USA*
[51]*Department of Physics, Tokyo Institute of Technology, Tokyo, 152-8551, Japan*
[52]*Institute of Physics, University of Tsukuba, Tsukuba, Ibaraki 305, Japan*
[53]*Vanderbilt University, Nashville, TN 37235, USA*
[54]*Waseda University, Advanced Research Institute for Science and Engineering, 17 Kikui-cho, Shinjuku-ku, Tokyo 162-0044, Japan*
[55]*Weizmann Institute, Rehovot 76100, Israel*
[56]*Yonsei University, IPAP, Seoul 120-749, Korea*

(Dated: February 8, 2008)

Two particle correlations between identified meson and baryon trigger particles with $2.5 < p_T < 4.0$ GeV/c and lower p_T charged hadrons have been measured at midrapidity by the PHENIX experiment at RHIC in p+p, d+Au and Au+Au collisions at $\sqrt{s_{NN}}$=200 GeV. The probability of finding a hadron near in azimuthal angle to the trigger particle is almost identical for leading mesons and baryons for non-central Au+Au. The yield for both trigger baryons and mesons is significantly higher in Au+Au than in p+p and d+Au, except for trigger baryons in central collisions. The baryon excess is likely to arise predominantly from hard scattering processes.

PACS numbers: 25.75.Dw

A remarkable feature of relativistic heavy ion collisions is greatly enhanced production of baryons and anti-baryons relative to mesons. This enhancement over elementary p+p collisions occurs at transverse momenta (p_T) of 2–5 GeV/c p_T [1, 2, 3]. In this range, particle production shifts from soft processes (non-perturbative, low momentum transfer scattering) to hard (high momentum transfer parton-parton scattering). Hard scattering is followed by fragmentation of the scattered partons to jets of hadrons. Baryon and anti-baryon production is suppressed in fragmentation. Phenomenologically, this can be thought of as a large penalty for creating a diquark/anti-diquark pair for baryon formation vs. a quark/anti-quark pair for meson formation.

Since there is no sharp separation of scales between hard and soft processes, it is natural to ask which is responsible for the baryon excess in Au+Au collisions. Hadron formation by recombination of boosted quarks from a collectively expanding source explains the observed baryon/meson ratios [4, 5, 6, 7]. The models include recombination of quarks from a thermal source, but the handling of hard partons varies significantly. Some allow hard parton fragmentation only, with no recombination [5]. Others model the distribution of shower partons in a jet, and allow soft and hard partons to coalesce [8]. These models should produce different hadron-hadron correlations in the recombination region, however quantitative predictions are not available. Baryon production by recombination of purely thermal quarks implies that the baryon excess is of soft origin, not from jet fragmentation. However, the yield of baryons in this momentum range scales approximately with the number of binary nucleon-nucleon collisions [2], which is typical of hard processes. Hadron production via recombination between jet fragments and thermal quarks [8] could preserve jet-like correlations among the final hadrons, presuming that each hadron contains at least one quark arising from a fragmenting hard scattered parton. As baryons contain one quark more than mesons, baryon production may be more strongly enhanced by the availability of additional quarks. Observation of such a mechanism would indicate modification of the jet fragmentation process by the medium produced in Au+Au collisions.

To determine the role of jets in the production of intermediate p_T protons, the PHENIX experiment at RHIC has measured energetic hadronic partners near the baryons. These are the additional fragmentation products from the same jet as the baryon. We present first results on two particle correlations where the *trigger* particle is an identified meson (π,K) or baryon (p,$\bar{p}$) at $2.5 < p_T < 4.0$ GeV/c. *Associated* particles, i.e. lower p_T charged hadrons, near in azimuthal angle to the trigger are counted. Momentum cuts are chosen to avoid contamination by resonance decays. The centrality and collision system dependence of the associated particle yield per trigger is used to help disentangle thermal quark recombination from jet fragmentation. Trigger particles from recombination of boosted thermal quarks should not have correlated partners beyond the expected correlation from elliptic flow. However, if the source of the baryons is indeed fragmentation of hard scattered partons, the probability of finding a jet-like hadronic partner should be comparable to that observed in p+p collisions. We use p+p collisions without trigger identification to provide a comparison baseline.

Data presented here include collisions at $\sqrt{s_{NN}} = 200$ GeV of Au+Au (24 million events), d+Au (42 million events) and p+p (23 million events). Charged particles are reconstructed in the central arms of PHENIX using drift chambers, each with an azimuthal coverage of $\pi/2$ and two layers of multi-wire proportional chambers with pad readout (PC1, PC3) [9]. Pattern recognition is based on a combinatorial Hough transform in the track bend plane, with the polar angle determined by PC1 and the collision vertex along the beam direction [1]. Particle momenta are measured with a resolution $\delta p/p = 0.7\% \oplus 1.0\% p$ (GeV/c) in Au+Au and $\delta p/p = 0.7\% \oplus 1.1\% p$ (GeV/c) in d+Au and p+p. The portion of the east arm spectrometer containing the high resolution Time-Of-Flight(TOF) detector, which covers pseudo-rapidity $|\eta| < 0.35$ and $\phi = \pi/4$ in azimuthal angle is used for trigger particle identification. Beam Counters (BBC) [9] provide the global start; stop signals are from TOF scintillators at a radial distance of 5.06 m. The timing resolution is $\sigma = 120$ ps, which allows a 4σ separation of mesons/baryons up to $p_T \approx 4$ GeV/c. The Au+Au centrality determination is described in Ref. [10].

Distributions of azimuthal angular difference, $\Delta\phi$, are constructed for trigger-partner pairs. The combinatorial

background is determined by constructing mixed events in two steps: the number of trigger and partner particles is determined by sampling the measured single particle multiplicity distributions in the relevant momentum and centrality ranges. Then the 3-momenta of particles in the mixed event are determined by sampling the measured trigger and partner momentum distributions. To correct for the limited acceptance of the PHENIX spectrometers, the real event $\Delta\phi$ distributions are divided by $\Delta\phi$ distributions from the mixed events, normalized to a constant angular aperture. The shape of this distribution retains effects of the PHENIX azimuthal acceptance, but has no true correlations. The partner yield is then corrected for the reconstruction efficiency, detector aperture and (for Au+Au only) detector occupancy [11]. No extrapolation is made to $|\eta| > 0.35$. Since d+Au and Au+Au collisions contain uncorrelated combinatorial background from other particles in the underlying event, the mixed event partner yield per trigger, after the same efficiency correction, is subtracted using the normalization determined by the convolution of the trigger and partner single particle rates.

Because mixing and subtraction is done in finite size centrality bins, the background distribution is biased toward the more central events within a bin, as they produce more particles. Consequently, the subtraction is corrected for the width of the centrality bins used for mixing: 5% in Au+Au and minimum bias in d+Au. The width of trigger and partner number within a centrality bin is determined from the measured centrality dependence of particle multiplicity in the relevant momentum region and particle species [10, 11, 12, 13]. This width implies larger fluctuations in the number of partners per trigger in mixed events, so the mixed event partner yields are increased accordingly. This correction modifies the background level by ≈0.2% in the most central and ≈25% in the most peripheral Au+Au collisions.

Elliptic flow causes an angular correlation in Au+Au unrelated to jet fragmentation, a background to this measurement. The elliptic flow correlation is removed by modulating the azimuthally uniform combinatorial background by $1+2v_2^{assoc}v_2^{trig}\cos(\Delta\phi)$, where v_2^{assoc} and v_2^{trig} are the v_2 values measured for the partner and trigger p_T ranges, respectively [14] where the reaction plane is measured by the BBC at $3 < \eta < 4$ minimizing the influence of jets in the v_2 values. Because the centrality binning in this analysis is finer than in [14] the p_T integrated centrality dependence is used to interpolate v_2 for collisions more central than 20%.

Systematic uncertainties in Au+Au and d+Au partner yields arise from uncertainties in the corrections for centrality bin width, systematic and statistical errors on v_2 [14] (Au+Au only), uncertainty in the background subtraction due to the event mixing technique, and uncertainty in the detector occupancy correction. The cross-contamination of mesons and protons is less than 5%.

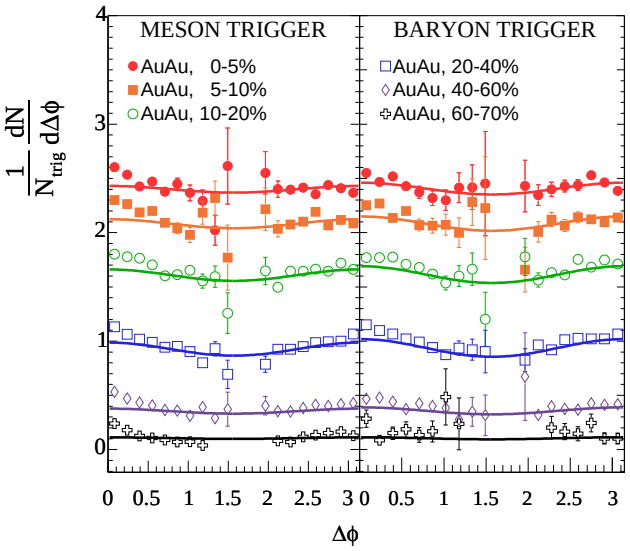

FIG. 1: $\Delta\phi$ distributions for meson (left) and baryon (right) triggers with $2.5 < p_T < 4.0$ GeV/c and associated charged hadrons with $1.7 < p_T < 2.5$ GeV/c for six centralities in Au+Au collisions. The solid lines indicate the calculated combinatorial background in the event modulated by the measured elliptic flow.

The error on the occupancy correction reaches a maximum of 5% in the most central Au+Au collisions. For most Au+Au bins, the dominant systematic uncertainty on the partner yields is the uncertainty in v_2. This produces a systematic error of approximately 0.01 partners per trigger baryon in semi-central and central collisions; for trigger mesons, the corresponding error is somewhat smaller. The event mixing uncertainty is approximately comparable to the v_2 uncertainty in these bins. In peripheral Au+Au collisions, the dominant systematic error in the partner yield arises from the centrality bin width corrections and v_2 uncertainty. In d+Au collisions, there is no v_2, and the partner yield uncertainty is driven by the correction for centrality bias of mixed events. In p+p collisions the systematic error is taken to be the same size as the combinatorial background which is subtracted. The total systematic errors are shown in Figure 2.

Figure 1 shows the $\Delta\phi$ distributions with trigger mesons (left) and baryons (right) measured at midrapidity ($|\eta|$ <0.35) in Au+Au collisions. The jet-like correlations are clearly visible over the combinatorial background, particularly at small relative angle inside the expected jet cone; the widths of the non-background distributions are consistent with jet fragmentation. The background is subtracted, and the number of associated partners per trigger integrated to determine the conditional yield of partners. The near (far) side yield is the integral over $0 < \Delta\phi < 0.94$ radians ($2.2 < \phi < \pi$ rad). The range is selected to include partners over as wide a range as possible, while omitting the limited acceptance region

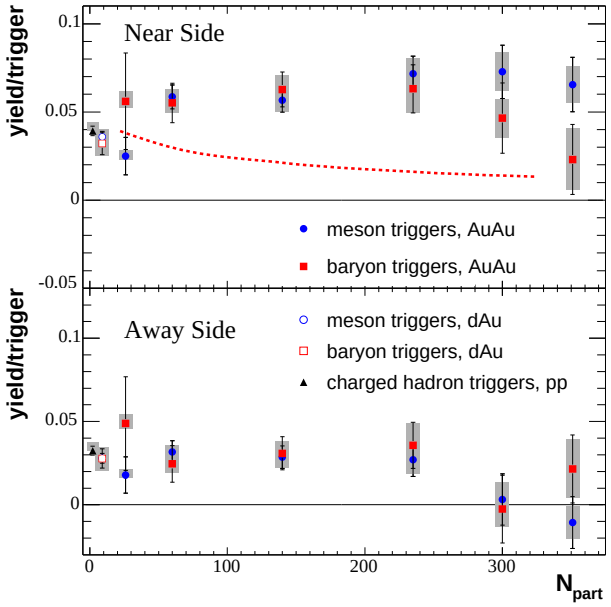

FIG. 2: Yield per trigger for associated charged hadrons between $1.7 < p_T < 2.5$ GeV/c for the near- (top) and away- (bottom) side jets. The error bars are statistical errors and the grey boxes are systematic errors. There is an additional 12% error on the overall normalization which moves all points together. The dashed line (top) represents an upper limit of the centrality dependence of the near-side partner yield from thermal recombination (see text).

around $\Delta\phi = \pi/2$. However, the non-background associated partners are observed in the angular range characteristic of jet fragmentation. The near side jet width in p+p collisions has been measured by PHENIX to be $\approx$ 0.25 rad in a similar p_T range [15].

Figure 2 shows the conditional yield per trigger of partner particles in p+p, d+Au, and Au+Au collisions, as a function of the number of participant nucleons. The top panel shows partner yield at small relative angle, from the same jet as the trigger hadron. We observe an increase in partner yields in mid-central Au+Au compared to the d+Au and p+p collisions; this almost doubling of the near side partner yield suggests that the fragmentation is modified by the medium. In Au+Au collisions, the near side yield per *meson* trigger remains constant as a function of centrality, whereas the near-side yield per *baryon* trigger decreases in the most central collisions as expected if a fraction of the baryons were produced by soft processes such as recombination of thermal quarks. In d+Au collisions the near-side yields per trigger are the same for meson and baryons triggers, and agree with results from p+p collisions generated with PYTHIA [16].

The dashed line in Figure 2 shows the expected centrality dependence of partners per baryon if all the "extra" baryons [10] which increase p/π over that in p+p collisions were to arise solely from soft processes. Baryons from thermal quark recombination should have no jet-like partner hadrons and would dilute the per-trigger conditional yield. Because this simple estimate does not allow for meson production by recombination, which must also occur along with baryon production, it represents an upper limit to the centrality dependence of the jet partner yield from thermal recombination. The data clearly disagree with both the centrality dependence and the absolute yields of this estimation, indicating that the baryon excess has the same jet-like origin as the mesons, except perhaps in the highest centrality bin.

The bottom panel of Figure 2 shows the conditional yield of partners on the away side. The partner yield in $2.2 < \Delta\phi < \pi$ rad drops equally for both trigger baryons and mesons going from p+p and d+Au to central Au+Au, in agreement with the observed disappearance [17] and/or broadening [15] of the dijet azimuthal correlations. It further supports the conclusion that the baryons originate from the same jet-like mechanism as mesons.

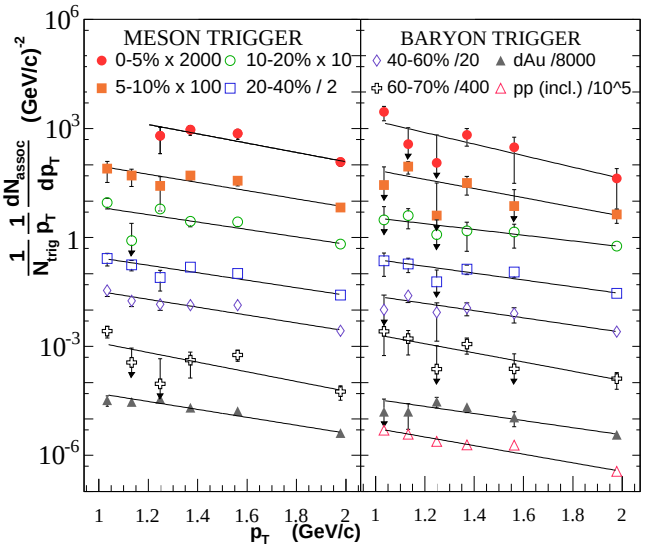

FIG. 3: p_T spectra of the near side associated charged hadrons corrected to the full jet yield for meson (left) and baryon (right) triggers at $2.5 < p_T < 4.0$ GeV/c and $|\eta| < 0.35$ for six centralities in Au+Au, d+Au and p+p collisions (non-identified trigger). Errors are statistical only. The curves are exponential fits. Inverse slope values are shown in Figure 4.

Figure 3 shows the p_T spectra of particles associated on the near side with trigger mesons and baryons. The measured transverse momentum of jet hadrons with respect to the inital parton direction, $\langle j_T \rangle$, is constant as a function of collision energy and p_T [15, 18]. Thus the angular size of jets increases as the partner p_T decreases. We used the PHENIX measurement of $\langle |j_{Ty}| \rangle = 0.359 \pm 0.011$ GeV/c [15] to correct the near side conditional yield measured in $\Delta\phi < 0.94$ rad and the PHENIX η acceptance to the full jet yield. This correction assumes

that jets are symmetric gaussians in both ϕ and η, and is required for the partner p_T spectra because of the p_T dependence of the jet width. The conditional yields in Figure 2 do not have this additional correction as they are measured in a single p_T bin. The partner spectra in Figure 3 are fitted with exponentials, and the slopes are given in Figure 4 as a function of N_{part}. The jet partner slopes exceed those of inclusive hadrons in the same p_T range [11], except perhaps in the most central collisions. The partner slopes are consistent between the collision systems and trigger type, indicating a common jet-like source for both baryons and mesons.

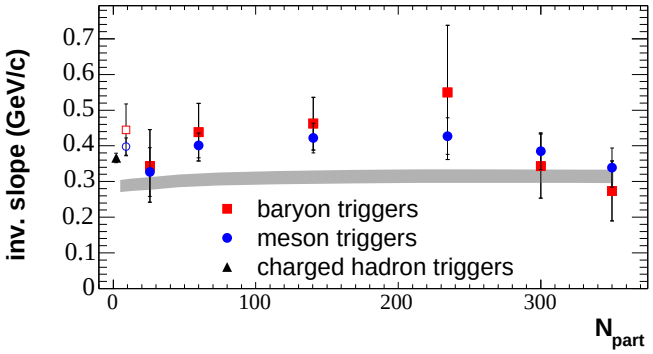

FIG. 4: Inverse slopes from the fits in Figure 3. Solid (hollow) squares and circles are Au+Au (d+Au) collisons and the triangle is p+p collisons. The solid band indicates the slopes of inclusive particle spectra in Au+Au collisions [11].

We have presented the first study of the jet structure of baryons $(p, \overline{p})$ and mesons (π, K) at midrapidity in Au+Au collisions at $\sqrt{s_{NN}} = 200$GeV, in the momentum region where baryon production is greatly enhanced in central Au+Au. Three observations indicate that mesons and baryons both arise predominantly from hard processes in all but the most central Au+Au collisions. First, baryons and mesons both have jet-like partner particles. Second, there is no strong change of the slope of the p_T spectra of associated particles from p+p to d+Au to Au+Au collisions, and it is larger than that of inclusive hadrons. Finally, on the away side, the jet partner yield into a 0.94 radian opening angle decreases in central collisions similarly for trigger baryons and mesons. The data are therefore inconsistent with a simple picture of baryon production at intermediate p_T dominated by recombination of only thermal quarks. On the trigger particle side, jets in Au+Au collisions are modified compared to those in p+p. They are richer in leading baryons and show enhanced probability for jet-like partners, except for the most central collisions with trigger baryons.

We thank the staff of the Collider-Accelerator and Physics Departments at BNL for their vital contributions. We acknowledge support from the Department of Energy and NSF (U.S.A.), MEXT and JSPS (Japan), CNPq and FAPESP (Brazil), NSFC (China), IN2P3/CNRS, CEA, and ARMINES (France), BMBF, DAAD, and AvH (Germany), OTKA (Hungary), DAE and DST (India), ISF (Israel), KRF and CHEP (Korea), RMIST, RAS, and RMAE (Russia), VR and KAW (Sweden), U.S. CRDF for the FSU, US-Hungarian NSF-OTKA-MTA, and US-Israel BSF.

* Deceased
† PHENIX Spokesperson:zajcnevis.columbia.edu

[1] K. Adcox *et al.*, Phys. Rev. Lett. **88**, 022301 (2002).
[2] S.S. Adler *et al.*, Phys. Rev. Lett. **91**, 172301 (2003).
[3] J. Adams *et al.*, Phys. Rev. Lett. **92**, 052302 (2004).
[4] C. Hwa and C. B. Yang, Phys. Rev. **C67** 034902 (2003).
[5] R. Fries, *et al.*, Phys. Rev. Lett. **90** 202303 (2003) and Phys. Rev. **C68**, 044902 (2003).
[6] V. Greco, *et al.*, Phys. Rev. **C68**, 034904 (2003).
[7] R. Fries, nucl-th/0403036 (2004).
[8] R. C. Hwa and C.B. Yang, nucl-th/0401001 (2004), and nucl-th/0403072 (2004).
[9] K. Adcox *et al.*, Nucl. Instrum. Methods **A499** 469 (2003).
[10] S.S. Adler *et al.* Phys. Rev. **C69**, 034909 (2004).
[11] S.S. Adler *et al.* Phys. Rev. **C69**, 034910 (2004).
[12] C. Klein-Bösing [PHENIX Coll.] nucl-ex/0403024.
[13] F. Matathias [PHENIX Coll.] nucl-ex/0403029.
[14] S.S. Adler *et al.* Phys. Rev. Lett. **91**, 182301 (2003).
[15] J. Rak [PHENIX Coll.] hep-ex/0403038.
[16] T. Sjöstrand *et al.* Comp. Phys. Comm. **135** 238 (2001).
[17] C. Adler *et al.*, Phys. Rev. Lett. **90** 082302 (2003).
[18] A.L.S. Angelis *et al.*, Phys. Lett. **B97** 163 (1980).